ELSEVIER

Physica B 240 (1997) 254–262

PHYSICA B

NMR study of intrinsic defects in congruent $LiNbO_3$. 1. "Unoverlapping" defects

A.V. Yatsenko[a], E.N. Ivanova[a], N.A. Sergeev[b,*]

[a] *Department of Physics, Simferopol State University, 333036 Simferopol, Ukraine*
[b] *Institute of Physics, University of Szczecin, ul. Wielkopolska 15, 70-451 Szczecin, Poland*

Received 17 January 1996; received in revised form 12 November 1996; accepted 17 February 1997

Abstract

The simulations of NMR spectra of ^7Li and ^{93}Nb nuclei for different models of intrinsic defects in single crystal of congruent lithium niobate have been performed. It has been shown that the most probable defects in $LiNbO_3$ are complex ($Nb_{Li} + 3V_{Li}$) and isolated V_{Li}. The NMR spectra of ^7Li have been simulated assuming that the potential surface of Li ion in the distorted LiO_6 octahedron has four minima.

Keywords: Intrinsic defects; NMR; $LiNbO_3$

1. Introduction

The intrinsic defects in lithium niobate (LN) crystals resulting from Li/Nb non-stoichiometry considerably change the optical, acoustical and other properties of LN. At present, it is believed that the excess of Nb^{5+} ions in congruent LN occupy only the regular Li sites [1–10]. The required local charge neutrality of LN can be guaranteed either by the oxygen vacancies [1], by Li vacancies at Li sites [2] or by Nb vacancies at Nb sites [3, 4]. The oxygen vacancy model [1] cannot explain the dependence of the density LN on the Li/Nb ratio [11] and thus is excluded. The Li-site vacancy model is supported by the X-ray and neutron diffraction studies [6, 12] and by computer simulations of defects energies [7, 8]. The Nb-site vacancy model is substantiated on the basis of an analysis of single crystal X-ray data [4] and on an NMR study [3]. Thus, it seems that at present a definite consensus on the intrinsic defect model in LN has not been achieved.

NMR is the method which allows to obtain direct local information about the real structure of the defects in crystals [13–15]. LN contains four different quadrupolar nuclei – ^{17}O (natural abundance is 0.037%; spin $I = \frac{5}{2}$ [15]), ^6Li (natural abundance is 7.42%; spin $I = 1$ [15]), ^7Li (natural abundance is 92.58%; spin $I = \frac{3}{2}$ [15]) and ^{93}Nb (natural abundance is 100%; spin $I = \frac{9}{2}$ [15]). The quadrupolar nuclei ^{17}O have very low natural abundance and NMR ^{17}O may be observed only on the enriched samples.

The NMR studies of ^7Li in LN have been reported in Refs. [16–24]. The temperature dependencies of the NMR spectra of ^7Li at $T > 450$ K indicate that Li ions diffuse onto the regular positions in LN (Schottky defects) [16, 20]. It is interesting to note that, to a good approximation, the $\Delta\nu$

*Corresponding author.

PII S0921-4526(97)00415-8

($\Delta\nu$ is the distance between the "quadrupolar" lines of ^{7}Li NMR spectrum [13–15]) depends linearly on the temperature of the sample in the interval 77–334 K and above 334 K [20]. At $T \approx 334$ K this dependence has a bend [20]. An analysis of the observed temperature dependencies of $\Delta\nu$ suggests that with increasing temperature the Li ion moves towards the lower oxygen plane [20]. The additional NMR lines in LN have been observed in [18, 21, 22]. The quadrupolar splitting $\Delta\nu$ of these weak lines is larger than that of basic "quadrupolar" lines in ratio 1.49. In order to explain these additional weak lines, Yatsenko et al. [18] assumed that in distorded LiO_6 octahedron there are some minima on the potential surface, which are occupied by Li ions with different probabilities. The calculations of the potential relief for Li ion in distorted LiO_6 octahedron show that the potential function has four minima: (a) three equivalent minima U_a shifted from *c*- axis and related by symmetry axis 3 and (b) one minimum U_b sited on *c*-axis [24]. From calculations it follows that $U_a < U_b$. Thus, we may assume that the basic lines in the NMR spectra of ^{7}Li may be related with those lithium nuclei which occupy the three minima U_a and the weak additional lines are related to the Li ions which occupy the potential minimum U_b [24]. The NMR spectra of ^{7}Li nuclei at $T = 4.2$ K support this model of multiminima potential of Li ion in the distorted LiO_6 octahedron [23]. The NMR of ^{6}Li was studied in Ref. [25]. By comparing the NMR data for ^{7}Li and ^{6}Li it has been shown that ^{6}Li nuclei occupy the sites only on the *c*-axis [25].

The NMR studies of ^{93}Nb in LN have been reported in Refs. [3, 19–21, 26–32]. All these reports mention the effect of the intrinsic defects in LN on the line shape of NMR ^{93}Nb observed in the asymmetry of the line shape of the central transition ($+\frac{1}{2} \leftrightarrow -\frac{1}{2}$ [13–15]). The additional NMR line of ^{93}Nb nuclei has been studied in Ref. [21]. However, this additional line was observed only in some crystals LN and, probably, is due to the defects of the crystal growth. MAS-NMR study of LN did not exhibit any additional line also [19]. In [30–32] the influence of the extrinsic paramagnetic defects and the influence of laser illuminations on the line shape of NMR ^{93}Nb in congruent $LiNbO_3$: Fe,Cu have been investigated.

For the interpretation of the observed line shape asymmetry of ^{93}Nb in LN two different methods have been proposed [33–36]. The first method [33] reconstructs the NMR line shape by familiar approach of image reconstruction from projections in NMR microscopy [37]. In spite of the limitations of this approach, it gives some qualitative information about the probability distribution of the components of electric field gradient (EFG) tensors at the sites of ^{93}Nb nuclei [33]. The second method uses the analysis of the angular dependencies of the first and second moments of the NMR central-transition line shapes [34–36]. This method also gives information only about the probability distribution of the components of EFG tensors at the sites of ^{93}Nb nuclei.

In this paper we have analysed the NMR spectra of ^{7}Li and ^{93}Nb using the simulations of the NMR spectra with different models of intrinsic defects in LN. The simulations have been performed assuming that (1) the intrinsic defects are distributed randomly in crystal lattice; (2) the distortions of lattice which may be introduced by the intrinsic defects are negligible; (3) the influence of two different defects on EFG tensors of ^{7}Li and ^{93}Nb is excluded ("nonoverlapping" defects). The effects of the lattice distortions and "overlapping" defects will be considered in the second part of paper [38].

2. Method of NMR spectra simulations

The calculations of the EFG tensors at the sites of nuclei require a preliminary knowledge of the so-called "effective" charges of lattice ions, antishielding factors $(1 - \gamma_\infty)$, precise coordinates of ions in crystal, etc. Moreover, in the case of ^{93}Nb nuclei, the covalence effects of chemical bonds Nb–O must be considered [27].

Common expression for EFG tensor components V_{kl} ($k, l = x, y, z$) in a crystal-fixed coordinate frame can be written as

$$V_{kl} = (1 - \gamma_\infty)(V_{kl})_{\text{latt}} + (V_{kl})_{\text{cov}}, \quad (1)$$

where $(V_{kl})_{\text{latt}}$ is the contribution to EFG tensor from the effective charges of lattice ions; $(V_{kl})_{\text{cov}}$ is the contribution to EFG tensor from the covalence

effects resulting from the overlapping electron shells of ions.

For the effective charges of ions we used the following effective charges: $q_{Li} = 0.98|e|$; $q_{Nb} = 3.67\ |e|$; $q_O = -1.55\ |e|$, which were obtained in Ref. [39] by direct calculation of the electron density in LN with the help of OLCAO method. Covalent contribution to EFG tensor of ^{93}Nb was calculated using three additional charges q_{ad} localized in the middle of the Nb–O bonds. The value of $q_{ad} = -0.039|e|$ was obtained by comparing the experimental one [27, 35] with the V_{ZZ} value (V_{ZZ} is ZZ-component of EFG tensor in the principal axes frame of EFG) for ^{93}Nb calculated in the pure ionic model. For ^{7}Li we used $(1-\gamma_\infty) = 0.744$ [27] and for ^{93}Nb - $(1-\gamma_\infty) = 16$ [27]. EFG tensors components were calculated in the same manner for all ^{7}Li and ^{93}Nb nuclei in the sphere with radius of 0.7 nm (centre of the sphere is at the site of the defect).

Because ^{7}Li nucleus has relatively small quadrupolar moment Q_{Li} ($Q_{Li} = -3.66\times10^{-26}$ sm^2 [15]), NMR spectrum of ^{7}Li can be described in a first order of the perturbation theory [13–15]. In this case NMR spectrum of ^{7}Li contains three lines with frequencies

$$\nu_0(\mathrm{Li}) - \Delta\nu, \quad \nu_0(\mathrm{Li}), \quad \nu_0(\mathrm{Li}) + \Delta\nu,$$

where $\nu_0(\mathrm{Li}) = \gamma_{Li}B_0$ (γ_{Li} is the gyromagnetic ratio of ^{7}Li nucleus) and

$$\Delta\nu = (eQ_{Li}V_{ZZ}/4\ \mathrm{h})(3\cos^2\theta - 1 + \eta\sin^2\theta\cos 2\varphi). \tag{2}$$

In Eq. (2) V_{ZZ} is the main component of EFG tensor of nucleus at site of ^{7}Li nucleus, $\eta = (V_{XX} - V_{YY})/V_{ZZ}$ is the asymmetry parameter of EFG tensor, XYZ is the principal axes frame of EFG tensor at the Li site. The angles θ and φ are the spherical angles of $\boldsymbol{B}_0$ direction in the XYZ axes frame.

The spin of ^{93}Nb nucleus is $\frac{9}{2}$ and NMR spectrum of ^{93}Nb must contain nine lines [13–15]. The presence of structural defects in LN leads to alteration of the ^{93}Nb EFG tensor both in magnitude and orientation. These alterations of the EFG tensor components at sites of nuclei ^{93}Nb are leading to the inhomogeneous broadening of the quadrupolar satellites line shapes and experimental NMR spectra of ^{93}Nb usually contain only one line (transition $+\frac{1}{2} \leftrightarrow -\frac{1}{2}$) [27, 29]. The frequency of this line ν is determined by the second-order quadrupolar effects and can be written as [40]

$$\nu = \nu_0(\mathrm{Nb}) - K[A(\varphi)\cos^4\theta + B(\varphi)\cos^2\theta + C(\varphi)]/(6\nu_0(\mathrm{Nb})), \tag{3}$$

where ν_0 (Nb) $= \gamma_{Nb}B_0$ (γ_{Nb} is the gyromagnetic ratio of ^{93}Nb) and

$$K = (3eQ_{Nb}V_{ZZ})^2[I(I+1) - \tfrac{3}{4}]/[2I(2I-1)h]^2, \tag{4}$$

$$A(\varphi) = -(\tfrac{27}{8}) + (\tfrac{9}{4})\eta\cos 2\varphi - (\tfrac{3}{8})\eta^2\cos^2 2\varphi,$$

$$B(\varphi) = (\tfrac{30}{8}) - 2\eta\cos 2\varphi - (\tfrac{1}{2})\eta^2 + (\tfrac{3}{4})\eta^2\cos^2 2\varphi, \tag{5}$$

$$C(\varphi) = -(\tfrac{3}{8}) - (\tfrac{1}{4})\eta\cos 2\varphi + (\tfrac{1}{3})\eta^2 - (\tfrac{3}{8})\eta^2\cos^2 2\varphi.$$

In Eq. (4) Q_{Nb} is the quadrupolar moment of ^{93}Nb nucleus ($Q_{Nb} = -37\times10^{-26}$ sm^2 [15]); $\eta = (V_{XX} - V_{YY})/V_{ZZ}$; V_{XX}, V_{YY}, V_{ZZ} are the components of the EFG tensor at the site of ^{93}Nb nucleus in the principal axes frame. The angles θ and φ describe the orientation of the magnetic field $\boldsymbol{B}_0$ in the XYZ-frame.

The simulations of NMR spectra of ^{7}Li and ^{93}Nb nuclei were fulfilled according to the following algorithm:

1. For a given type of the intrinsic defects the EFG tensors at the sites of nuclei Li and Nb in the sphere ($R = 2$ nm) have been calculated in a crystal-fixed coordinate frame;
2. By the diagonalization of $V_{kl}^{(i)}$ tensors (i – the number of the EFG tensor) the array of the values ($V_{ZZ}^{(i)}$, $\eta^{(i)}$, $\theta^{(i)}$, $\varphi^{(i)}$) have been obtained;
3. Then the calculated values of $V_{ZZ}^{(i)}$, $\theta^{(i)}$ were assumed as expected values of respective Gaussian distributions functions with standard deviations $\sigma(V_{ZZ}^{(i)}) = 0.03\ V_{ZZ}^{(i)}$ and $\sigma(\theta^{(i)}) = 2^0$. This assumption allows partly to take into account the distortions of the lattice which are introduced by the intrinsic defects;
4. Each $V_{kl}^{(i)}$ from the array of values ($V_{ZZ}^{(i)}$, $\eta^{(i)}$, $\theta^{(i)}$, $\varphi^{(i)}$), by means of equation (2) for ^{7}Li (or Eq. (3) for ^{93}Nb) allows to obtain the frequencies of NMR spectrum;
5. Taking into account the concentration of the given type of intrinsic defects and broadening of the

each line of spectrum by the Gaussian functions (its second moment equal to the Van-Vleck second moment [14, 15]), the simulated NMR spectra have been obtained.

3. Results and discussion

The experimental NMR spectra have been obtained at the room temperature using the home-built wide-line NMR spectrometer with the stabilized Pound–Knight detector. To increase the signal to noise ratio (SNR) the 2048-channel digital averager has been used [41]. Measurements were made at $B_0 = 1.13$ T for ^{7}Li NMR and at $B_0 = 1.4$ T for ^{93}Nb NMR. Experimental results have been obtained on undoped congruent LN single crystals and on the Fe-doped (0.07 wt%) samples. The NMR spectra of ^{7}Li and ^{93}Nb for undoped and Fe-doped crystals of LN have the same shapes. Predicted types of the intrinsic defects in LN [1–4] and their modifications according to a local electroneutrality principle are presented in Table 1.

Single crystals of the congruent LN were grown by the Czochralski method and were obtained from the different Laboratories of Russia (Novosibirsk, Sankt-Petersburg, Moscow).

The results of simulations and experiments are shown in Figs. 1 and 2. From Figs. 1 and 2 we see that models (a)–(f) cannot describe the experimental NMR spectra of ^{7}Li and ^{93}Nb nuclei in LN. The discrepancy between the simulated and experimental NMR spectra are caused probably by the local distortions of the lattice introduced by the defects. The local distortion of lattice, so as the influence of the "overlapping" defects on the EFG

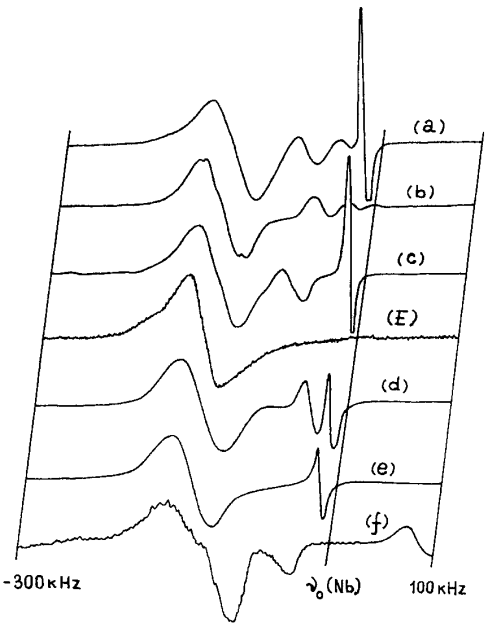

Fig. 1. Experimental (E) and simulated ((a)–(f)) NMR spectra of ^{93}Nb nuclei for different models of the intrinsic defects in LN. $\alpha = 35°$. α is the angle between $\boldsymbol{B}_0$ and crystal axis of symmetry $\boldsymbol{c}$.

Table 1
Models of intrinsic defects in congruent LN[a]

Chemical formula (48.4% Li_2O)	Models of defects[b] and distributions of defects in lattice	Symbol of model
$Li_{0.9371}$ Nb $O_{2.9686}$ [1]	Random distribution of $6V_{Li}$ and $3V_O$	(a)
	Random distribution of 3 complexes $V_O + 2V_{Li}$	(b)
$[Li_{0.947}$ $Nb_{0.0106}]$ NbO_3 [2]	Random distribution of Nb_{Li} and $4V_{Li}$	(c)
	Random distribution of complex $Nb_{Li} + 3V_{Li}$ ($3V_{Li}$ are sited above Nb_{Li}) and V_{Li}	(d)
	Random distribution of complex $Nb_{Li} + 3V_{Li}$ ($3V_{Li}$ are sited below Nb_{Li}) and V_{Li}	(e)
$[Li_{0.947}$ $Nb_{0.053}]$ $Nb_{0.9576}$ O_3 [4]	Random distribution of 4 complexes ($Nb_{Li} + V_{Nb}$) and Nb_{Li}	(f)

[a] V_{Li}, V_O, V_{Nb} – vacancies of Li, O and Nb ions, respectively; Nb_{Li}–Nb ion on Li-site.
[b] per 100 formular units approximately.

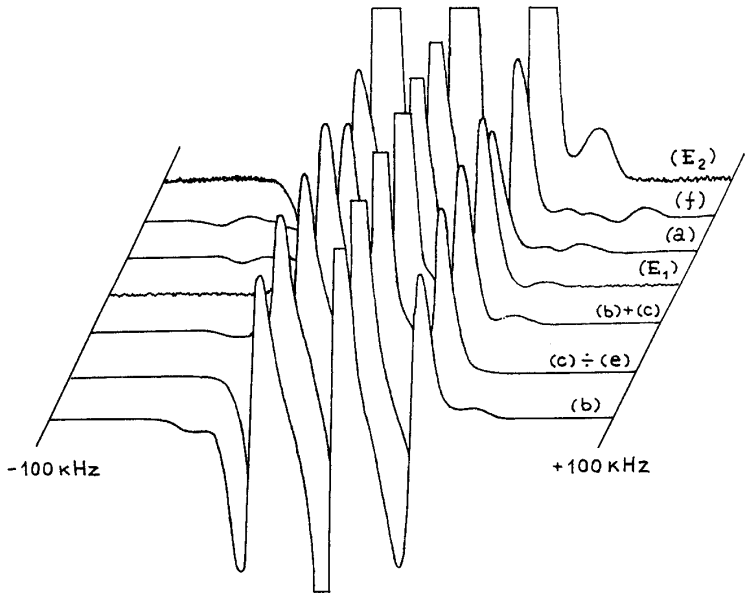

Fig. 2. Experimental (E_1 and E_2) and simulated ((a)–(f)) NMR spectra of ^{7}Li nuclei for different models of the intrinsic defects in LN. $\alpha = 0°$.

tensors, must increase the alteration of the components of the EFG tensors on the sites of nuclei Li and Nb. These alterations of the EFG tensors must lead to the inhomogeneous broadening of the spectral lines so that the additional lines in NMR spectra of ^{93}Nb (Fig. 1) may vanish. The additional inhomogeneous broadening of the NMR spectra will increase the second moment of NMR spectra of ^{93}Nb also. From data shown in Fig. 3 and in Table 2 we may conclude that only models (d) and (e) of the intrinsic defects in LN the models (d) and (e) are close to the NMR experimental data.

The simulated NMR spectra of ^{7}Li nuclei (Fig. 2) for the models (a), (b) and (f) contain the weak additional lines just in the ranges where the additional "quadrupolar" lines are observed. It is interesting to note that the simulated spectra for the models (b) + (c) with relative concentrations 1.1 : 1 are in good agreement with the experimental spectra not only qualitatively but also quantitatively (Fig. 4).

However, as can be seen from Fig. 2, for the models (d) and (e), which preferably describe the experimental data on ^{93}Nb NMR, the NMR spectra of ^{7}Li do not contain any additional "quadrupolar" lines. Our experimental data show that the shapes of the NMR spectra of ^{7}Li in LN do not change for high enough concentrations of the impurity (up to 0.7 wt% of Fe and up to 2 wt% Mg). It may be suggested that the additional lines in experimental NMR spectra of ^{7}Li nuclei are not due to the intrinsic defects.

In order to explain these additional lines we assumed that, as mentioned in Introduction, the Li ions may occupy the four positions in the lattice of LN (Fig. 5). The results of the potential surface calculations for Li ion in the distorted LiO_6 octahedron have been reported in [24]. From these calculations it follows that the coordinates of those four minima are: a_1 (28 pm, 0 pm, 0 pm), a_2 (−14 pm, 24.25 pm, 0 pm), a_3 (− 14 pm, −24.25 pm, 0 pm), b (0, 0, −1.5 pm) (Fig. 5). If we

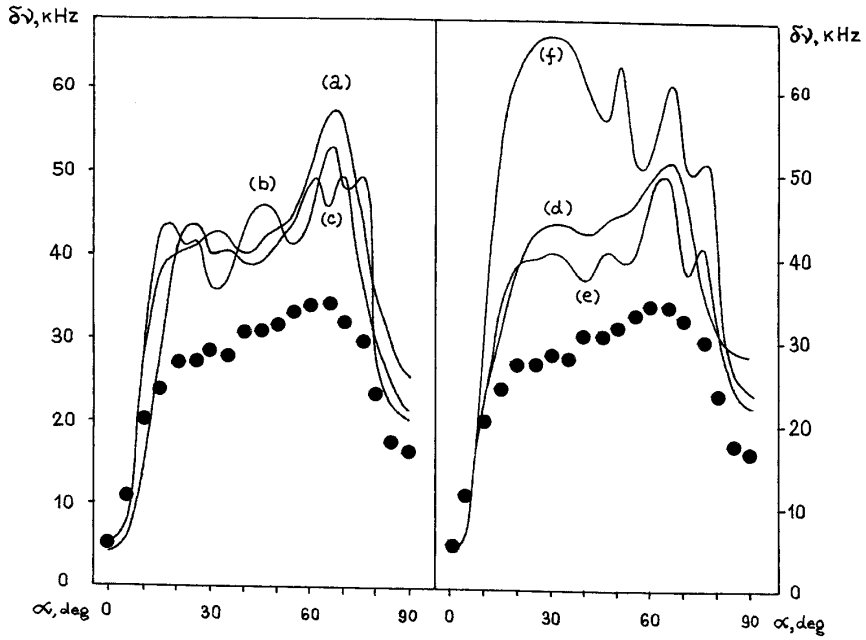

Fig. 3. Experimental (●) and calculated from the simulated spectra angular dependencies of the linewidth $\delta\nu$ of the NMR ^{93}Nb central transition line.

Table 2
Theoretical and experimental values of M_2 for central lines of ^{93}Nb NMR spectra. α is the angle between $\boldsymbol{B}_0$ and crystal axis of symmetry $\boldsymbol{c}$

Model	M_2 (kHz^2)			
	$\alpha = 0^0$	$\alpha = 35^\circ$	$\alpha = 60^\circ$	$\alpha = 90^\circ$
(a)	20.0	782	640	337
(b)	13.8	804	912	259
(c)	22.6	786	950	299
(d)	12.3	510	706	201
(e)	14.8	678	680	327
(f)	85.8	1965	977	585
Experimental	33 ± 2	2000 ± 100	⩾ 2000	430 ± 25

assume that Li-ion, occupying one of the a_i positions ($i = 1, 2, 3$), undergoes the fast reorientation about its threefold axis (axis $\boldsymbol{c}$), then it is easy to show [14, 15] that the quadrupole satellites splitting $\Delta\nu_1$ (Fig. 5(a)) of ^{7}Li NMR may be written as

$$\Delta\nu_1 = (eQ_{\mathrm{Li}}V_{ZZ}^{(a)}/4h)(3\cos^2\alpha - 1). \quad (6)$$

In Eq. (6) $V_{ZZ}^{(a)}$ is the main component of EFG tensor at sites of a_i ($i = 1, 2, 3$), α is the angle between the axis $\boldsymbol{c}$ and $\boldsymbol{B}_0$.

For Li ion which occupies the b-position on the symmetry axis $\boldsymbol{c}$ and is not mobile ($|U_a - U_b \gg kT$, Fig. 5(c)), we have from Eq. (2)

$$\Delta\nu_2 = (eQ_{\mathrm{Li}}V_{ZZ}^{(b)}/2h)(3\cos^2\alpha - 1), \quad (7)$$

where $V_{ZZ}^{(b)}$ is the major component of EFG tensor at b-site.

Using the coordinates of a_i and b positions, we calculated $V_{ZZ}^{(a)}$ and $V_{ZZ}^{(b)}$. Results of the calculations $\Delta\nu_1$ and $\Delta\nu_2$ are shown in Table 3. From Table 3 we see that there is a good quantitative agreement between computed and experimental data.

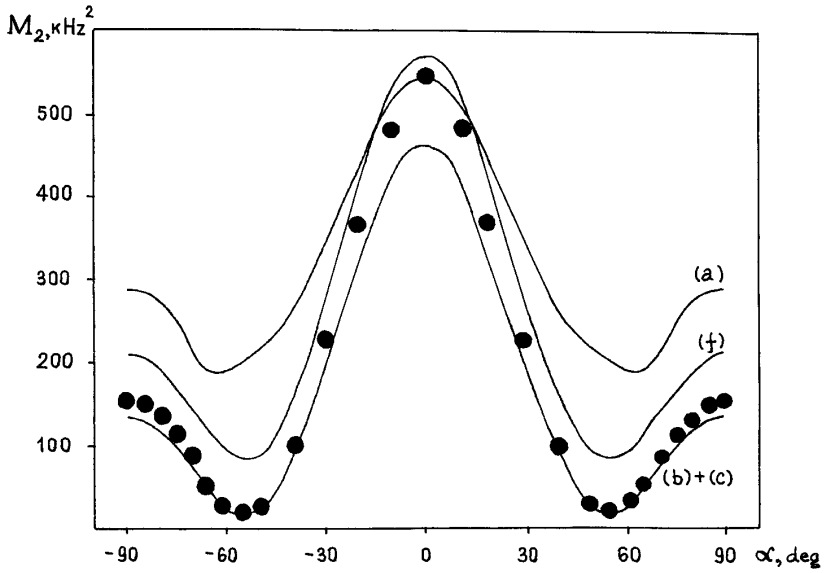

Fig. 4. Experimental (●) and obtained from the simulated spectra angular dependencies of the second moment M_2 of ^{7}Li NMR spectra.

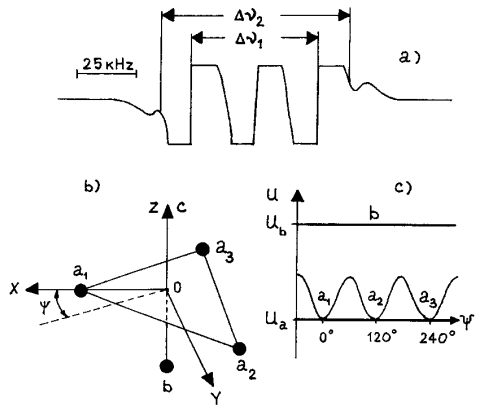

Fig. 5. (a) Experimental NMR spectrum of ^{7}Li at $\alpha = 0°$. (b) Scheme of the four equilibrium positions (a_1, a_2, a_3 and b) for Li-ion in LN. The position of the center O coincides with the positions of Li-ion defined by X-ray data [4]. Distances $Oa_1 = Oa_2 = Oa_3 = 28$ pm; $Ob = -1.5$ pm [24]. (c) Scheme of the potential function for the Li-ion in LN. $|U_b - U_a| \approx 0.075$ eV.

Table 3
Experimental and calculated values of $\Delta\nu_1$, $\Delta\nu_2$ and W_2/W_1

	Calculated	Experimental
$\Delta\nu_1$ (kHz)	54.7	55.0 ± 0.2
$\Delta\nu_2$ (kHz)	76.2	82.0 ± 2.0
$\Delta\nu_2/\Delta\nu_1$	1.39	1.49 ± 0.04
W_2/W_1	0.04	0.06 ± 0.01

Assuming the probabilities W_1 and W_2 of the occupations by Li ions of a_i and b positions as described by the Boltzmann distribution we may write

$$W_1/W_2 = \exp(-|U_a - U_b|/kT). \quad (8)$$

The experimental and calculated values of W_1/W_2 are also shown in Table 3. The calculations of W_1/W_2 have been performed using the theoretical data for potential surface obtained in

[24]. From data of Table 3 it follows that at $T = 300$ K

$$|U_a - U_b| \approx (7, 5)\,10^{-2}\ \text{eV}. \quad (9)$$

4. Conclusions

The presented results on the simulations of ^{7}Li and ^{93}Nb NMR spectra in congruent LN can be considered as preliminary ones since the influences of the "overlapping" defects and lattice distortions on NMR spectra still are not fully accounted. However, from these preliminary results it follows that the Nb-site vacancy model is not consistent with the NMR data and probably only the Li-site vacancy model may be considered as the proper intrinsic defect model of the LN structure. The investigations of NMR spectra of ^{7}Li nuclei show that the shapes of the resonance lines are not sensitive to the type of the intrinsic defects and the observed additional NMR lines of ^{7}Li in LN are probably related to the peculiarities of the potential surface and to the mobility of Li ions in the distorted LiO_6 octahedron.

Acknowledgements

The authors are indebted to Professor Ya.I. Granovskii for critical reading of the manuscript and for helpful discussions. We wish to express our gratitude to the referee for his valuable comments.

References

[1] W. Bollmann, Cryst. Res. Technol. 18 (1983) 1147.
[2] P. Lerner, C. Legras, J.P. Dumas, J. Cryst. Growth 3-4 (1968) 231.
[3] G.E. Peterson, A. Carnevale, J. Chem. Phys. 56 (1972) 4848.
[4] S.C. Abrahams, P. Marsh, Acta Cryst. B 42 (1986) 61.
[5] N. Zotov, F. Frey, H. Boysen, H. Lehnert, A. Hornsteiner, B. Strauss, R. Sonntag, H.M. Mayer, F. Güthoff, D. Hohlwein, Acta Cryst. B 51 (1995) 961.
[6] N. Iyi, K. Kitamura, F. Izumi, J.K. Yamamoto. T. Hayashi, H. Asano, S. Kimura, J. Solid. St. Chem. 101 (1992) 340.
[7] H.J. Donnerberg, S.M. Tomlinson, C.R.A. Catlow, O.F. Schirmer, Phys. Rev. B40 (1989) 11909.
[8] H.J. Donnerberg, S.M. Tomlinson, C.R.A. Catlow, J. Phys. Chem. Solids 52 (1991) 201.
[9] Y. Watanabe, T. Sota, K. Suzuki, K. Kimamura, S. Kimura, J. Phys.: Condens. Matter 7 (1995) 3627.
[10] O.F. Schirmer, O. Thiemann, M. Wöhlecke, J. Phys. Chem. Solids 52 (1991) 185.
[11] L. Kovács, K. Polgár, Cryst. Res. Technol. 21 (1986) K101.
[12] N. Zotov, H. Boysen, F. Frey, Th. Metzger, E. Born, J. Phys. Chem. Solids 55 (1994) 145.
[13] M.H. Cohen, F. Reif, in: Solid St. Physics, vol. 5, Academic Press, New York, 1957.
[14] A. Abragam, The Principles of Nuclear Magnetism, Oxford University Press, New York, 1961.
[15] J.W. Hennel, J. Klinowski, Fundamentals of Nuclear Magnetic Resonance, Longman Scientific and Technical, Harlow, 1993.
[16] T.K. Halstead, J. Chem. Phys. 53 (1970) 3427.
[17] L. Baiqin, W. Yening, X. Ziran, J. Phys. C: Solid St. Phys. 21 (1988) L251.
[18] A.V. Yatsenko, N.A. Sergeev, Ukr. J. Phys. 30 (1985) 118.
[19] J. Blümel, E. Born, Th. Metzger, J. Phys. Chem. Solids 55 (1994) 589.
[20] A.V. Yatsenko, Russ. Phys. Solid St. 37 (1995) 2203.
[21] A.V. Yatsenko, E.N. Ivanova, Russ. Phys. Solid. St. 37 (1995) 2262.
[22] A.V. Yatsenko, E.N. Ivanova, N.A. Sergeev, in Abstracts of the X National Conference Molecular Crystals, Kiekrz, Poland, 1995, p. P14.
[23] L.V. Dmitrieva, A.V. Yatsenko, in: Abstracts of XXIX Meeting on Low Temperature Physics, vol. 3, Kazan, Russia, 1992, p. T76.
[24] A.V. Yatsenko, N.A. Sergeev, in: Extended Abstracts of 28th Congress AMPERE, University of Kent, England, 1996, p. 279.; E.N. Ivanova, N.A. Sergeev, A.V. Yatsenko, Ukr. J. Phys. 42 (1997) 47.
[25] A.V. Yatsenko, in: Extended Abstracts of 28th Congress AMPERE, University of Kent, England, 1996, p. 281.
[26] G.E. Peterson, P.M. Bridenbaugh, J. Chem. Phys. 46 (1967) 4409.
[27] G.E. Peterson, P.M. Bridenbaugh, J. Chem. Phys. 48 (1968) 3402.
[28] G.E. Peterson, J.R. Carruthers, J. Solid State Chem. 1 (1969) 98.
[29] A.V. Yatsenko, V.N. Shcherbakov, S.P. Gabuda, Bull. Magn. Res. 2 (1980) p. 197.
[30] A.V. Yatsenko, N.A. Sergeev, Sov. Phys. Solid St. 27 (1985) 1239.
[31] A.V. Yatsenko, N.A. Sergeev, Sov. Phys. Solid St. 28 (1986) 2567.
[32] A.V. Yatsenko, N.A. Sergeev, Ukr. J. Phys. 33 (1988) 1101.
[33] D.C. Douglass, G.E. Peterson, V.J. McBrierty, Phys. Rev. B40 (1989) 10694.
[34] A.V. Yatsenko, N.A. Sergeev, Kristallografja, 35 (1990) 108.

[35] E.N. Ivanova, A.V. Yatsenko, N.A. Sergeev, Solid St. NMR 4 (1995) 381.
[36] A.V. Yatsenko, E.N. Ivanova, N.A. Sergeev, in: Abstracts of XVI Conference on Radio- and Microwave Spectroscopy RAMIS'95, Poznan, Poland, 1995, p. P-68.
[37] P.T. Callaghan, Principles of Nuclear Magnetic Resonance Microscopy, Clarendon Press, Oxford, 1991.
[38] A.V. Yatsenko, E.N. Ivanova, N.A. Sergeev, Physica B (to be published).
[39] W.Y. Ching, Gu Zong-Quan, Xu Yong-Nian, Phys. Rev. B 50 (1994) 1992.
[40] G.E. Jellison, S.A. Feller, P.J. Bray, J. Magn. Res. 27 (1977) 121.
[41] A.V. Yatsenko, V. Yu. Kornienko, Ukr. J. Phys. 41 (1996) 650.